Statistical Considerations in Linear Elastic Fracture Mechanics

Edward Mark Lenoe,* Donald M. Neal,† and I. Spiridigliozzi‡
Army Materials and Mechanics Research Center, Watertown, Mass.

Critical defect size distributions are estimated for various metals and for hot pressed silicon nitride using the Monte Carlo method. With regard to the critical flaw size computation, results obtained for the numerous materials are compared to the sensitivity or probability of detection of particular flaw sizes based on existing nondestructive evaluation techniques. In several instances, defect detection is the limiting factor. Comparison of flaw estimates for the silicon nitride to fractographic observations demonstrates capability of order of magnitude accuracy. The technique is also used to explore the influence of variable parameters in a simple crack growth law. An important result was the nonnormality of life estimates, even though normal distributions were used for input variables. The consequence is a much lower probability of occurrence for the modal value of the life distribution than might be anticipated. With regard to the Monte Carlo method, the paper demonstrates that selection of the appropriate number of simulations must rely on consideration of third and higher order moments of the resulting statistical distributions. A large number of simulations were needed in order to obtain convergence of these moments. This, in turn, provides criteria for required number of simulations in the defect size and life computation. In summary, the paper illustrates the importance of statistically based fracture mechanics materials selection criteria. Furthermore, it demonstrates that the simple series approximation technique generally underestimates mean values and variance, particularly for large variances in operating stress and materials properties. Most importantly, the technique provides probability distributions for realistic fatigue life estimates.

Introduction

REQUIREMENTS for high-performance materials operating in extreme environments have generally lead to the necessary use of high strength and brittle materials. Many of these materials possess excellent resistance to fatigue crack initiation. However, many advanced materials, due in part to their limited production base, often inherently contain severe internal or initial manufacturing defects which can enlarge at an alarming rate in comparison to the fatigue crack initiation stage. Then, too, their generally low fracture resistance renders these materials far more susceptible to potential catastrophic brittle failure. It is imperative to explore more systematically the fracture mechanics characteristics in the selection and application of tougher materials than has been done previously.

In this paper, inherent critical materials defects are emphasized rather than those structural details which can drastically amplify the stress-range intensity. Application of fracture mechanics involves a sequence of operations, starting with establishment of the initial flaw size, choice of failure criteria, estimates of the number of cycles required for the initial flaw size to reach critical or inspectable flaw size, and finally, an overall comparison of these characteristics for the candidate materials. Usually these computations are treated on a deterministic basis, and conservative parametric values are the basis of estimated behavior. In this case, we treat the matter from a statistical viewpoint by considering the influence of variation in the materials' parameters by means of the Monte Carlo method.

Received September 19, 1974; revision received February 11, 1975. The support of the Advanced Research Projects Agency is acknowledged. In particular, the authors express their gratitude to E. C. VanReuth of ARPA. The painstaking and efficient manuscript preparation of A. Travers is also sincerely appreciated.

Index categories: Reliability, Quality Control, and Maintainability; Structural Design, Optimal; Materials, Properties of.

*Chief, Mechanics of Materials Division.

†Senior Research Mathematician. Member AIAA.

‡Engineering Aide.

Monte Carlo Method

The Monte Carlo method is a desirable means of determining flaw sizes since the controlling parameters, e.g. K_{IC}, σ_{ult}, and σ are inherently variable. The relative complexity of the functional relationship, in addition to the expense of extensive experimentation, further suggests the need for the Monte Carlo method. The method avoids restrictions on the exact specification of the statistical distributions of the variables, since simple approximating functions can serve well in the scheme. In general, this prevents formulation of incorrect frequency distributions for the quantities of interest.

In this paper, determination of critical crack radius a_{cr} by the Monte Carlo method involves representing each of the independent variables by a set of normally distributed random numbers. Use of normal distributions is not a requirement. However, due to resulting simplifications, normal distributions were used in this initial phase of our work. The pertinent equation, including plasticity corrections, commonly applied for defect size estimates is

$$a_{cr} = K_{IC}{}^2 \left[\phi^2 - 0.212\left(\frac{\sigma}{\sigma_{ult}}\right)^2\right]/1.21\,\pi\sigma^2 \qquad (1)$$

where K_{IC} = fracture toughness, σ = operating stress, σ_{ult} = ultimate strength, and ϕ = stress intensity factor for appropriate crack geometry.

A value is specified for each variable by choosing a number at random from its corresponding distribution. The resulting value for a_{cr} is determined for each set of randomly selected variables. The computation is repeated and a probability distribution is obtained for the defect sizes.

The normally distributed random numbers were generated by a Univac 1108 subroutine. The procedure is simply one of generating uniform random numbers and solving for X in the relation

$$\int_{-\infty}^{X} f_i\,dx = R \qquad (2)$$

where R = uniform random number and f_i = normal frequency distribution. As noted previously, if the probability distributions of the controlling variables are known

Table 1a Summary of critical flaw size determinations—typical aerospace metals, 60% yield strength, ±15% variation

Materials	K_{IC} [ksi(in)$^{1/2}$]	Yield strength (ksi) (0.2%)	Critical flaw radius, in.			
			Monte Carlo (400 trials)		Taylor series approximation	
			Interior flaw	Surface flaw	Interior flaw	Surface flaw
4340 steel	53 ± 2.8	240 ± 15	0.096 ± 0.03525	0.0545 ± 0.0204	0.0864 ± 0.02824	0.04895 ± 0.0163
18N$_i$, maraging steel	68.4 ± 3.51	257 ± 17.7	0.1397 ± 0.0511	0.07936 ± 0.02962	0.1258 ± 0.04101	0.0713 ± 0.02374
Titanium						
6Al-4V	109.3 ± 4.5	140 ± 10	1.209 ± 0.4342	0.687 ± 0.2515	1.0902 ± 0.3490	0.6170 ± 0.2022
mill range	230.4 ± 8.4	140 ± 10	5.372 ± 1.912	3.0515 ± 1.11	4.8442 ± 1.5398	2.746 ± 0.8922
Aluminum						
2024-T3	106.8 ± 5	42 ± 3.5	13.4698 ± 4.882	7.658 ± 2.827	12.1366 ± 3.918	6.888 ± 2.269
2024-T4	44.1 ± 3.8	42 ± 3.5	2.3101 ± 0.9173	1.3134 ± 0.53	2.069 ± 0.7321	1.1744 ± 0.4225
7075-T6	50.9 ± 7.2	70 ± 4.1	1.1244 ± 0.521	0.6394 ± 0.3	0.994 ± 0.4164	0.5642 ± 0.24
7178-T6	46.4 ± 5.1	75 ± 6.0	0.81164 ± 0.343	0.46155 ± 0.20	0.7235 ± 0.2743	0.4107 ± 0.1580

Table 1b Summary of critical flaw size determinations—typical aerospace metals, 25% yield strength, ±15% variation

Materials	Critical flaw radius, in.			
	Monte Carlo (400 trials)		Taylor series approximation	
	Interior flaw	Surface flaw	Interior flaw	Surface flaw
4340 steel	0.5658 ± 0.2035	0.3276 ± 0.118	0.5104 ± 0.163	0.295 ± 0.0946
18N$_i$, maraging steel	0.8217 ± 0.2946	0.4749 ± 0.171	0.7414 ± 0.2362	0.4283 ± 0.137
Titanium				
6Al-4V	7.0627 ± 2.481	4.082 ± 1.438	6.38 ± 1.994	3.686 ± 1.156
mill range	31.37 ± 10.92	18.13 ± 6.33	28.35 ± 8.8	16.38 ± 5.1
Aluminum				
2024-T3	75 ± 26.6	43.3 ± 15.4	67.7 ± 21.4	39.1 ± 12.4
2024-T4	12.85 ± 5.02	7.43 ± 2.91	11.54 ± 4.0	6.7 ± 2.32
7075-T6	6.24 ± 2.86	3.61 ± 1.65	5.53 ± 2.28	3.2 ± 1.32
7178-T6	4.48 ± 1.87	2.59 ± 1.08	4.0 ± 1.5	2.31 ± 0.87

Table 2 Flaw radius estimates[a]—hot pressed silicon nitride (deterministic value for mean = 0.0052)

σ Percent standard deviation	Monte Carlo method		Series Approx.	% Difference	
	Mean	S.D.	S.D.	Mean	S.D.
1	0.0055	0.0027	0.0027	6	0.0
3	0.0055	0.0028	0.0028	6	0.0
5	0.0056	0.0029	0.0028	8	4
7	0.0056	0.0030	0.0029	8	3
9	0.0057	0.0031	0.0029	10	7
11	0.0057	0.0033	0.0030	10	10
13	0.0058	0.0035	0.0031	11	13
15	0.0060	0.0038	0.0032	15	19

[a] K_{IC} = 3.2 ksi (sq. in., S.D. = 0.8557; ϕ^2 = 2.5 (internal spheroidal flaw); σ_{ult} = 59.17 ksi, S.D. = 7.45; σ = 35.5 ksi (operating stress).

from some experimental results or from an analytical basis, then the appropriate distribution function f_i may be used in Eq. (2).

Flaw Size Estimates

Variables that affect fracture toughness, limitations of experimental procedures, and statistical analysis of fracture toughness data of engineering alloys have been discussed by several investigators.[1,2] Lin,[1] for example, compared normal, two- and three-parameter lognormal and two- and three-parameter Weibull distributions for fracture toughness data and suggested that the two-parameter lognormal function would generally satisfactorily reproduce experimental data. The functions were compared on the basis of rms differences, and examination of these rms values indicated it would not be unreasonable to approximate the K_{IC} values by normal distributions. Therefore, typical mean values and standard deviations for K_{IC} data on aerospace materials were selected[1,2] and the Monte Carlo method was applied to Eq. (1). The flaw size estimates were completed for two levels of operating stress (25 and 60% of σ_y) and assuming variability in the operating stress ranging up to ±15%. The results of the initial calculations, for 400 simulations, are summarized in Table 1. Note both the mean values and standard deviations (S.D.'s) are tabulated.

Using silicon nitride, the means and S.D.'s for certain variances of the operating stress are presented in Table 2. A comparison of results for the Monte Carlo and series approximation is also presented. In determining the S.D. using the series approximation method as a first-order Taylor series approximation, the following relationship is used.

$$\delta = \left[\sum_i^n \left(\frac{\partial Z}{\partial x_i} \right)^2 \delta_{x_i}{}^2 \right]^{1/2} \tag{3}$$

where δ = S.D. (standard deviation), x_i = independent variable (e.g., K_{IC}), δ_{x_i} = S.D. independent variable, and Z = dependent variable (a_{cr}). It is apparent that the series approximation generally underestimates both means and S.D.'s.

Results for the Monte Carlo method in Table 1 are for 400 simulations and are therefore relatively crude computations. Equation (1) was systematically evaluated for 4340 steel and for hot-pressed silicon nitride. To effectively determine the proper number of simulations, the behavior of third and fourth moments of the flaw size distribution was surveyed as a function of increasing number of trials. It was found that the mean and standard deviation were not sufficient for examining effects of number of simulations since the shape of the calculated distribution

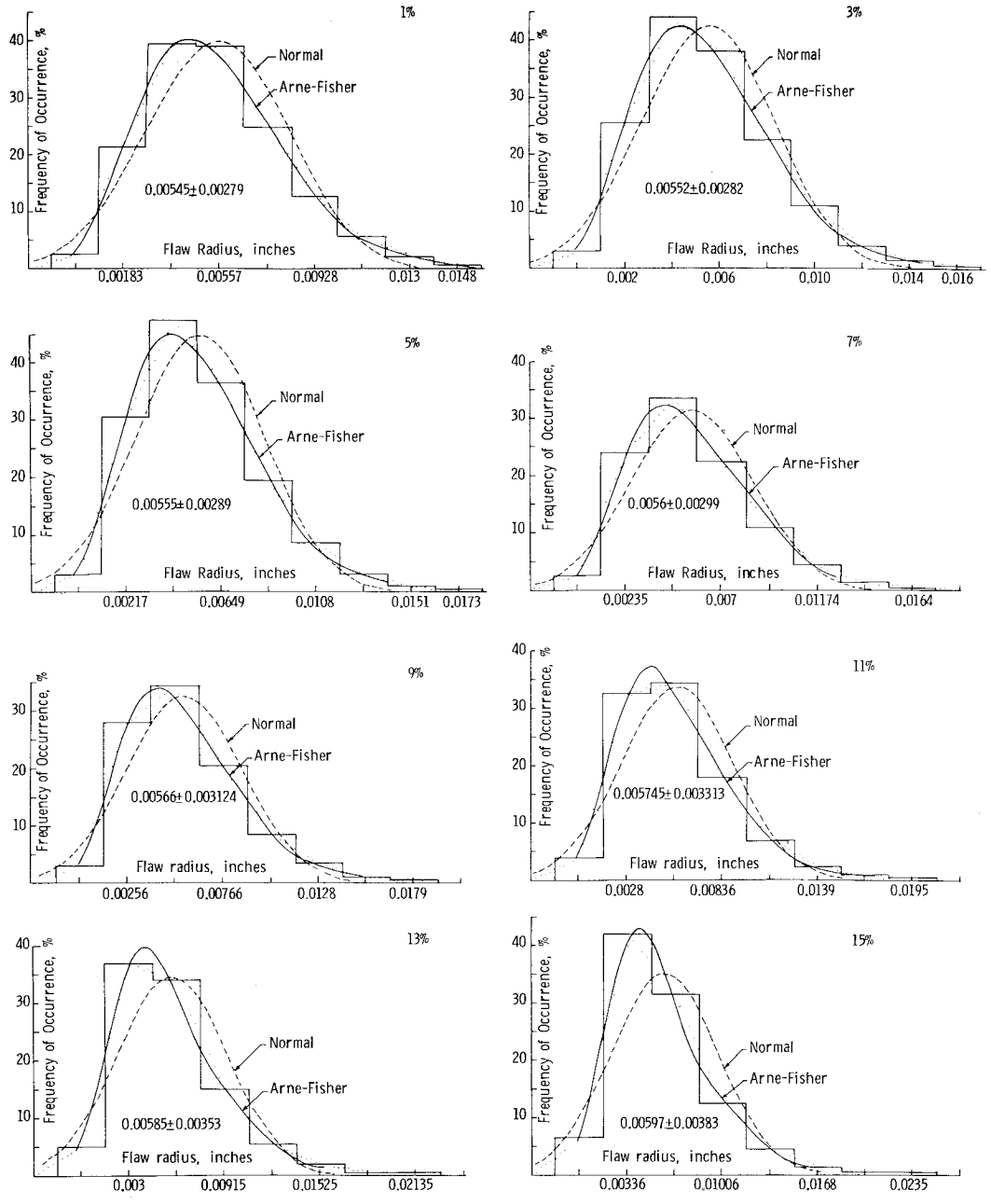

Fig. 1 Monte Carlo estimates of flaw size distribution for silicon nitride.

function continued to change, long after constant first and second moments had been achieved. The number of trials were systematically increased up to 8000 simulations. Using the error analysis[3] $E = [3\delta/(N)^{1/2}]$ where E = error, δ = S.D., and N = number of trials, resulted in errors of the order of 0.0001 for $N = 8000$.

The measure of quality of fit, referenced to the normal distribution, was the Kolomogorov coefficient.[4] In general, the silicon nitride material did not have an acceptable normal distribution, and was skewed somewhat to the right.

An attempt was made to fit the flaw histograms with lognormal functions, but error was too great. An acceptable distribution function was determined by using the Arne Fisher[5] least-square fit approach. This employs an equation of the form

$$f(X_i) = \sum_{j=o}^{p} C_j D_y^j[\Phi(y)] \qquad (4)$$

where $C = j$th Arne Fisher coefficient with $j = 0,1, \ldots$; f = frequency; X_i = data point; $\bar{X}$ = mean; δ = S.D.; $y = [(X_i - \bar{X})/\delta]$; $D^j[\Phi(y)] = j$th derivative; $\Phi(y) = [\exp(-y^2/2)]/(2\pi)^{1/2}$; and P = number of terms plus one.

To simplify the computation, the following relation may be substituted for Eq. (4):

$$f(X) = \sum_{j=0}^{p} C_j H_j(y)\Phi(y)$$

with the Hermite polynomials H_j defined as $H_0(y) = 1$, $H_1(y) = y$, and

$$H_{r+1}(y) = y[H_r(y) - rH_{r-1}(y)]$$

with

$$r = 1, 2, \ldots$$

using a value of $P = 7$, produced a satisfactory frequency distribution function for the Monte Carlo estimates, as depicted in Fig. 1, for the various standard deviations in operating stress.

It is of interest to compare the results of the Monte Carlo estimates summarized in Table 2 to those obtained using the series approximation, e.g. $\bar{a}_{cr} = 0.0052$ and $\delta_{acr} = 0.0028$. We obtained generally good agreement, with maximum differences of 15%. Once again, however, the series approximation ordinarily underestimated means and variances.

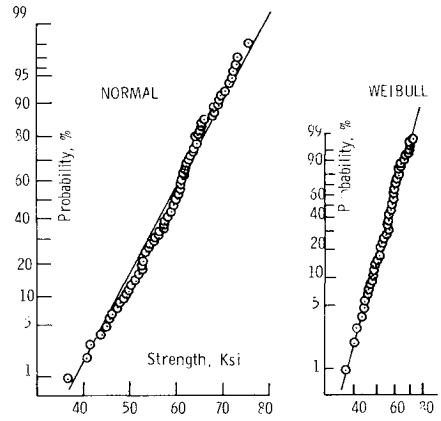

Fig. 2 Tensile strength of hot pressed silicon nitride (NC-130) compared to statistical distributions.

Regarding the flaw size estimates, probability density functions of the independent variables were based on available experimental data. The tensile strength distributions, for instance were fit to ring hydroburst results[6,7] as well as to data obtained on conventional contoured tension specimens.[8] The Weibull and normal distributions are compared to the experimental observations on hot-pressed silicon nitride in Fig. 2.

Fractographic analysis of mechanical properties specimens of hot pressed silicon nitride have been carried out by a number of investigators.[8,9] Baratta, et al.[8] carried out scanning electron microscopy to determine location and size of fracture initiating flaws for room temperature tension and flexure response while Baumgartner and Richerson[9] performed similar microscopy of four-point flexure specimens. Their results are shown in Fig. 3. Of interest is the range in mean flaw radii (0.00053–0.00124 in.) compared to the calculated value of ~0.0055 for nominal operating stresses of 67% of the strength of the material, suggesting that conventional linear elastic fracture mechanics is capable of estimating the correct order of magnitude of flaw size in this brittle material. Considering the nature of the defects, this is rather remarkable agreement, due to the difficulty of accurately idealizing the fracture origins as spherical or even elliptical voids. Figure 4, for example, illustrates typical low-density flaw sites. At higher magnifications, it is evident there is no clear demarkation of the defects and obviously idealized spherical flaw sizes would vary considerably with individual judgment exercised during examination of photo micrographs.

The detailed examination of specimens with internal or subsurface fracture origins indicated that for tensile specimens, fractures generally initiated in such typical regions of incomplete densification, containing large amounts of interconnected porosity. Inclusions or second phases were

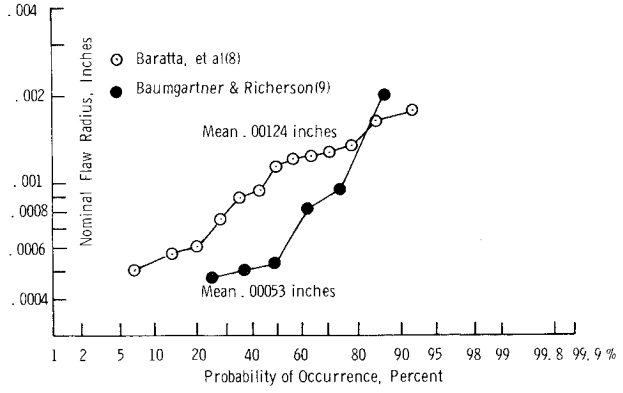

Fig. 3 Experimentally determined critical flaw sizes in hot-pressed silicon nitride.

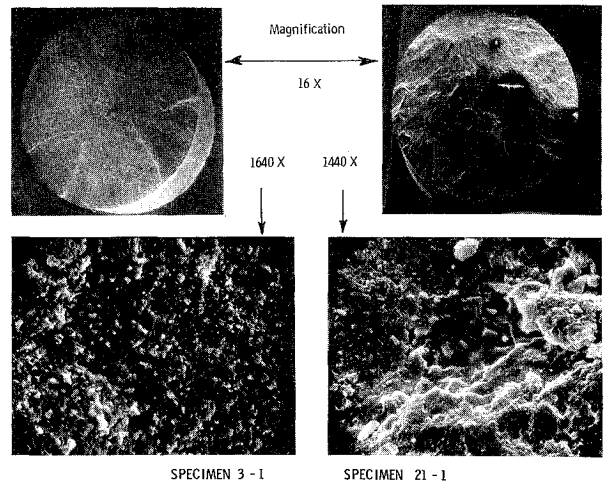

Fig. 4 Scanning electron micrographs of typical porous flaws in hot-pressed silicon nitride.

also observed to initiate subsurface fracture in both tensile and flexure specimens. In the hot pressed materials examined here, there was a tendency for elements such as Ca, V, Mn, Co, Ba, and in some instances Fe, to preferentially segregate to the porous fracture site. In second-phase particles or inclusions which were not fracture initiation sites, Al, Mo, Ca, and Fe have been observed.[8] However, based on limited data, it is premature to attribute the high porosity-low density regions of fracture origin to specific impurities.

With regard to flaw size distributions, it is of interest to consider the defect estimates for other materials. Figure 5 presents the distribution for 4340, while Fig. 6 displays the computations for beryllium. Referring to Fig. 5, the defect estimates are rather closely approximated by a normal distribution. There is only slight suggestion of skewness. The higher ratio of fracture toughness (K_{IC}) to design stress (σ), as contrasted to the silicon nitride material, apparently tends to diminish nonnormality.

Beryllium is of interest for several reasons. More than a decade ago a major beryllium turbine engine development program was jointly initiated in the United States and the United Kingdom (Ref. 10, p. 87). Design studies had indicated potential weight saving of 70% in blades and 60% in compressor disks as contrasted to titanium. Major problems encountered in this program were failure of blades under impact and brittle failures of disks, which led to termination of the beryllium turbine engine development program.

Consideration of fracture data[11-13] reveals that about 80% of the K_{IC} results for beryllium lie between 10–25 ksi(in)$^{1/2}$. Although there is a tendency for fracture toughness to decrease with increasing thickness, scatter in avail-

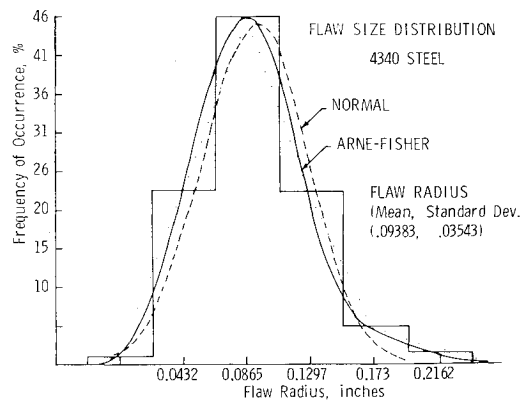

Fig. 5 Flaw-size estimates for steel.

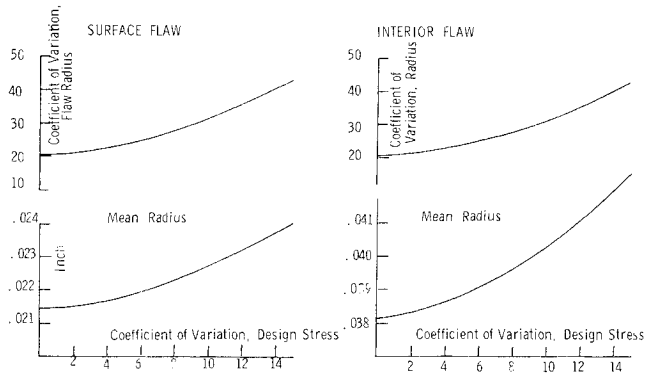

Fig. 6 Flaw-size estimates for beryllium; strength = 59.2 ± 1.2, fracture toughness 9.78 ± 1.06, design stress 40 ksi.

able data is too large to positively identify such an effect. For computations reported here, input data was somewhat arbitrarily taken as $\sigma_{ult} = 59.2 \pm 1.2$, $K_{IC} = 9.78 \pm 1.06$.

The strength data is based on the histograms illustrated in Fig. 7. An overall comparison of flaw size estimates for the different materials is made in Fig. 8, using 95% confidence limits for the estimated mean values. The comparisons are made for assumed interior spherical flaws and nominal operating stresses at 60% of yield, ±15%. In all the Monte Carlo computations, it was assumed that the flaw location was known and the geometric factor was assumed constant.

Figure 9 summarizes the results for the silicon nitride in terms of the variation and mean flaw radius as a function of coefficient of variation in design stress. Note that in this instance, the variance in K_{IC} and σ_{ult} were 26.7 and 12.6%, respectively. While the variance for the ultimate strength is representative of the material, it is likely that the scatter in fracture toughness data will be reduced as experimental procedures are further developed.

Crack Propagation Estimates

Past studies of fatigue crack propagation in metals have lead to an extensive literature dealing with component fatigue life prediction. Hoeppner and Krupp,[14] for example, summarize and discuss 33 proposed crack propagation relations, while other investigators present numerous variants of such laws.[15-19] One of the more common of fatigue crack propagation relationships for metals is of the form

$$(da_{cr}/dN) = C(\Delta K)^m \qquad (6)$$

where now m is taken as a material constant, ΔK is the range of stress intensities, and N represents the number of fatigue cycles. Freudenthal[19] has indicated that based on

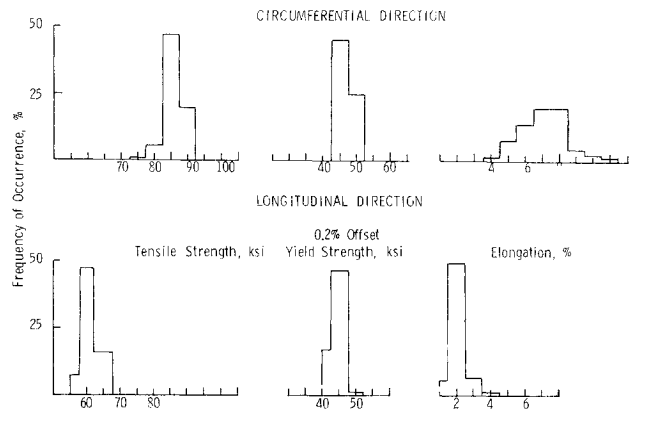

Fig. 7 Typical strength distributions for beryllium.

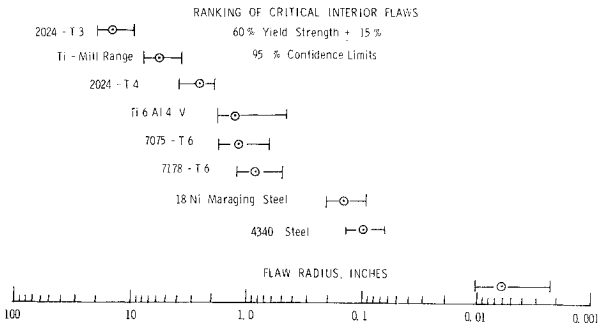

Fig. 8 Flaw-size estimates for various materials (95% confidence limits).

crack growth experiments, the material constant m seems to vary within the limits $2 < m < 10$, where high values of $5 < m < 10$ are characteristic for high strength metals and for crack propagation under fully plastic conditions of ductile metals. Lower values of $2 < m < 5$ represent crack propagation against elastically restrained plastic resistance. Integration of Eq. (6) between limits of initial crack or flaw size a_{cr} and the terminal crack size is the basis of the life estimate.

Usefulness of Eq. (6) depends on reliability of knowledge of C, ΔK, and m, as well as the correctness of the assumptions that crack growth depends on stress range alone and is nearly independent of the mean stress. It is known that in order to encompass the entire range of crack propagation, including initial and terminal stages, propagation rules other then Eq. (6) are required. However, in the middle range of fatigue crack growth, the equation is reasonable although scatter ranges of about 1:3 in crack growth rates are representative of reported slow crack growth measurements. For purposes of discussion, crack growth in 4340 steel and time to failure predictions in hot-pressed silicon nitride have been considered.

Data for crack propagation in steel[20] were used to consider the case of fatigue life of a landing gear, treated in a deterministic manner by Krupp and Hoeppner.[21] The fracture mechanics analysis was for a 4340 steel main landing gear part, from a typical large transport or bomber aircraft. The service life requirement was 6000 flights under a service spectrum whose peak stress was 78.5 ksi. Crack growth in the main landing gear component from an initial length of 0.075 to a critical length of 0.606 in. was estimated at 7550 flights, significantly larger than the target 6000 missions. Using similar mean values, and the indicated standard deviations for independent variables,

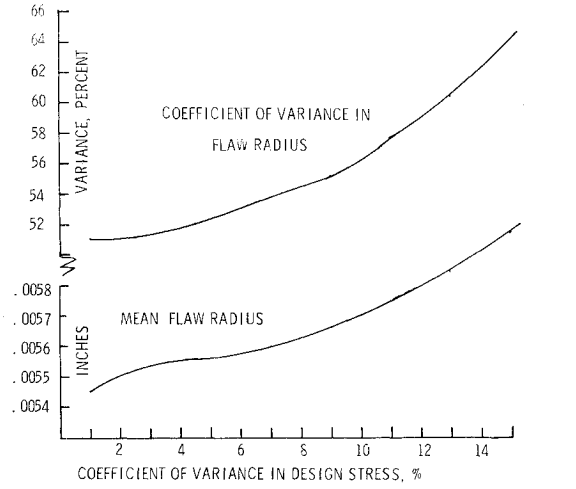

Fig. 9 Estimated flaw sizes for hot-pressed silicon nitride; yield strength 59.17 ± 7.46, fracture toughness 3.2 ± 0.86, design stress 35.5 ksi.

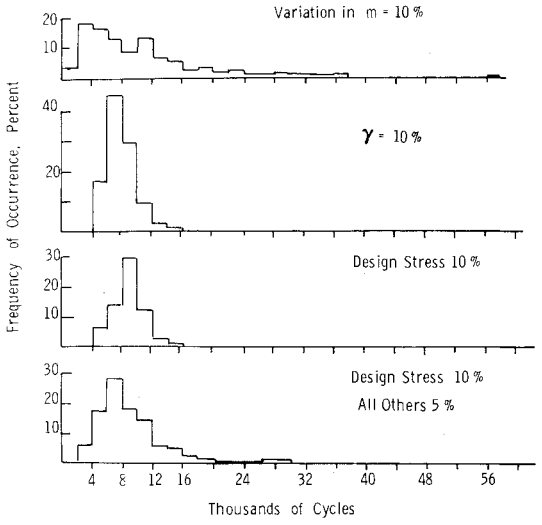

Fig. 10 Illustrative sensitivity of fatigue life estimates to variance of controlling parameters.

Eq. (6) was solved by performing necessary integration and then applying the Monte Carlo method. A number of computations were completed in order to investigate sensitivity of the crack growth equation to statistical distributions of the controlling variables. These computations involve reasonable variations in the parameters $C = 1.09 \times 10^{-8}$, $m = 2.17$, $\Delta\sigma = 78.5$ ksi and $\gamma = 0.85$ over the range of crack length 0.025–0.202 in. as shown in Fig. 10. Histograms where each variable was allotted a coefficient of variance of ±10% with all other variables assumed constant are also illustrated. The results of the sensitivity analysis to the various input parameters are shown in Fig. 10, for 400 simulations. It is evident that the exponent m, is the quantity causing most scatter, resulting in a multimodal and highly skewed fatigue life distribution. This indicates a greater need for careful evaluation of m. Of further interest is Fig. 11, for the case of typical coefficients of variance in controlling parameters. The distribution is again highly skewed. In order to obtain a more accurate estimate, the number of trials was increased by 6000 and the final results are compared in Fig. 11. It is evident that the modal value is associated with a fairly low probability of occurrence. Longer as well as shorter fatigue lives possess a significant probability of occurrence.

Time-to-Failure Predictions for Silicon Nitride

In many metals, the concept of fatigue crack growth and its relation to the physical basis of the crack propagation rate (da/dN) rule is easily clarified by means of fractographic analysis of mechanically stressed components. Fatigue striations are often clearly displayed in a fractograph of the failed component. A precise determination

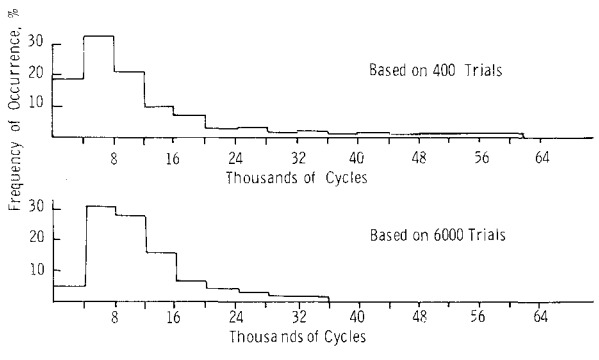

Fig. 11 Monte Carlo fatigue life estimates for main landing gear.[21]

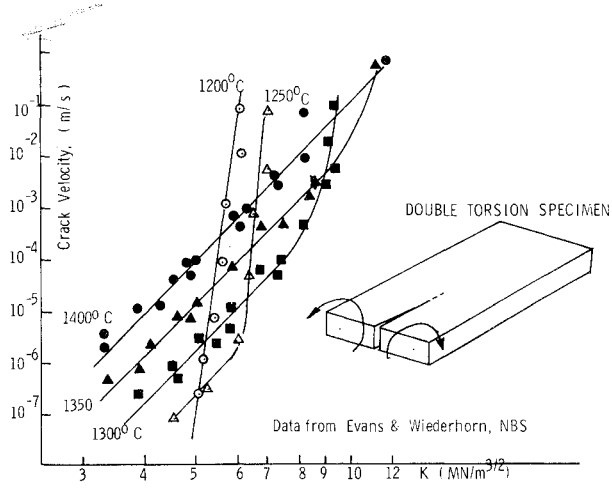

Fig. 12 Crack growth rate vs stress intensity, hot-pressed silicon nitride.

can then often be made of the number of fatigue cycles on the basis of direct measurements of these striations. Due to a lack of detailed knowledge concerning the mechanisms of fatigue in structural ceramics, such direct approaches are not presently available.

Evans and Wiederhorn[22] have described the techniques for generating and applying slow crack growth data to ceramics in order to predict failure. Due to the difficulty of crack growth measurements at elevated temperature, several specific experimental techniques have evolved. Use of the double-torsion configuration (see schematic in Fig. 12) under quasi-static conditions has enabled measurement of crack velocity behavior as a function of nominal stress intensity level. The specimen has been used in several modes to obtain crack growth rate information: fixed displacement, constant displacement rate, or constant load. The most prevalent is the fixed displacement mode which yields continuous crack growth rate data using the double torsion configuration. Both displacement and load amplitudes have been employed with sinusoidal cycles and frequencies <5 Hz. For this range of observation there do not appear to be significant frequency effects. However, further experimentation is required for a comprehensive evaluation of crack growth in ceramics.

Several applications of Eq. (6) have been made to estimate the life of ceramic components.[23-27] In one instance, the crack velocity relationship is integrated directly to obtain a time to failure t_f, with m, C_o, and K_o determined from crack velocity V vs K_I results, then the form is

$$t_f = \frac{2}{C_0(n-2)\sigma^2\phi^2}\left[\frac{1}{K_{Ii}^{n-2}} - \frac{1}{K_{IC}^{n-2}}\right] \tag{7}$$

An alternate formulation is based on the Weibull strength distribution

$$P_f = 1 - \exp[-(S/S_o)^m] \tag{8}$$

where $S = [K_{IC}/\phi(a_o)^{1/2}]$ and S_o and m are the Weibull constants, and substituting into Eq. (6), under constant stress conditions, the failure time becomes

$$ln\ t = (n-2)/m\ ln\ ln[1/(1-P_f)] - n\ ln\sigma + ln\ S_o + ln\left[\frac{2}{C_o(n-2)\phi^2 K_{IC}^{n-2}}\right] \tag{9}$$

The Monte Carlo technique was applied to Eq. (6), using crack velocity data from Fig. 12. Even for low stress levels, the estimated life times for the silicon nitride were found to be comparatively short at the 2500°F temperatures. In order to improve service life, proof test procedures have been advocated in the past as well as recently.[27] For proof test conditions, denoting σ_p as the over proof stress and σ_a as the applied or service stress, the

minimum life estimate now becomes

$$t_{\min} = \left[\frac{2}{(n-2)C_o\sigma_a^2\phi^2(K_{IC})^{n-2}}\right]\left[\left(\frac{\sigma_p}{\sigma_a}\right)^{n-2}\right] - 1 \quad (10)$$

With regard to Fig. 12, it should be noted that the data are for an early generation of hot-pressed silicon nitride. Later, higher purity materials promise higher strength but tougher components. In attempting to carry out life estimates, it is prudent to briefly consider the strength distribution function Eq. (8) which is an important aspect of the analysis.

In the engineering literature, Eq. (8) is referred to as the Weibull distribution since he suggested its application to describe material fracture strength.[28] It is widely accepted that the brittle fracture strength of a material under a homogeneous stress state is related to its defect structure, and the concentration and severity of these defects. Equation (8) is general in character and assumes the inhomogeneities are uniformly distributed over the volume of the body. Alternate formulations have been proposed to describe strength. The statistical approach to brittle fracture has been fairly thoroughly reviewed,[29] and current alternate approaches seek to incorporate physically relevant probability models for the controlling fracture mechanisms. A theoretical justification for a multiple-fracture process involving Griffith cracks has been proposed by Gilvarry.[30] McClintock[31] hypothesized the existence of intergranular cracks related to microstructural details and computed frequency distributions of cracks as a function of size.

Other researchers have also sought to further develop theories in which fracture is due to intergranular cracks and voids[32-34]; Batdorf, for instance, has considered a weakest link theory for isotropic materials containing randomly oriented microcracks uniformly distributed throughout the volume. Then the strength statistics are given by

$$P_f = 1 - \exp\left[-V\int_o^\infty \frac{\Omega(\Sigma,\sigma_{cr})}{4\pi}\frac{dN}{d\sigma_{cr}}\,d\sigma_{cr}\right] \quad (11)$$

where Ω represents the solid angle containing the normals to all orientations for which the component of the applied stress normal to the crack plane is $\sigma_n > \sigma_{cr}$, and Σ signifies the applied stress state in an element of volume ΔV of a materials with crack density N.

Then under the assumption of cracking for normal stresses

$$\frac{\Omega}{4\pi} = 1 - \left(\sqrt{\frac{\sigma_{cr}}{\sigma}}\right) \text{ for uniaxial stress } \sigma_{cr} < \sigma$$
$$= \left(\sqrt{1 - \frac{\sigma_{cr}}{\sigma}}\right) \text{ for equibiaxial stress}$$
$$= 0 \text{ for } \sigma_{cr} > 0 \quad (12)$$

N can be expanded in Taylor series and inserted into Eq. (11). The resulting expression for P_f (σ) is then fitted to laboratory uniaxial data to arbitrary precision. Then fracture statistics for other stress states are obtained from Eq. (11) with appropriate choice of Ω (Σ,σ_{cr}).

For small s (where s = effective stress), then

$$P_f = 1 - \exp\left[-VN_0(S^4/4)\exp(-1/S^4)\right] \quad (13)$$

This theory is incomplete since it assumes fracture is determined by the tensile stress normal to a crack plane and cannot account for fracture in pure compression. In effect this assumption takes account of direct stresses acting on a crack, but neglects the effect of shear, which is only justifiable when the maximum compressive stress is less in absolute value then three times the maximum principal feasible stress. Note that for materials with low dispersion in fracture stress, this theory reduces to a form similar to that of Weibull.

An alternate form based on different crack formation and size distribution hypothesis[34] for simple tension is

$$P_f(S) = 1 - \exp\left[-VN_o\int_o^S\left(1 - \frac{X}{S}\right)\frac{4}{S^5}\exp^{-1/X^4}dX\right]$$

where

$$S = \sigma\frac{2A^{1/4}}{K_I(\pi^3|ln|\,9)^{1/4}} \quad (14)$$

A = grain cross section, and K_I = fracture toughness.

In terms of comparing different fracture theories, earlier studies[35] resulted in a suggested room temperature, two-parameter Weibull strength distribution for the hot-pressed silicon nitride as

$$P_f = 1 - \exp\left[-0.693\left(\frac{\sigma}{96}\right)^{10.86}\right] \quad (15)$$

Batdorf,[36] assumed the existence of 1600 microcracks, plus 4 cracks near a stress concentration of 1.85 and suggested the probability distribution

$$P_f = 1 - \exp[-1600\,F(S) - 4F(1.85)]$$

where

$$F(S) = \int_o^S\left(1 - \frac{X}{S}\right)\frac{4}{S^5}\exp^{-1/X^4}dX \quad (16)$$

Comparison of these two distributions illustrates one of the frustrations of research in the field of brittle fracture statistics since available experimental results are generally insufficient to clearly choose one theory as opposed to another. However it would seem desirable to use theories which successfully reproduce observed size effects, which can be related to microstructural details and which can incorporate known surface (microcracking due to machining) effects.

However, because of the typical wide scatter of ceramic strength and the general unavailability of high-temperature strength data, we are currently more-or-less forced to deal with the less elegant theories and to rely on proof testing and nondestructive flaw detection in order to enhance component life.

Probability of Flaw Detection

The control as well as the prediction of flaws occupies a predominant role in use of fracture mechanics analysis for fatigue and fracture failure.[37] Quality control in materials processing and component manufacture, periodic nonde-

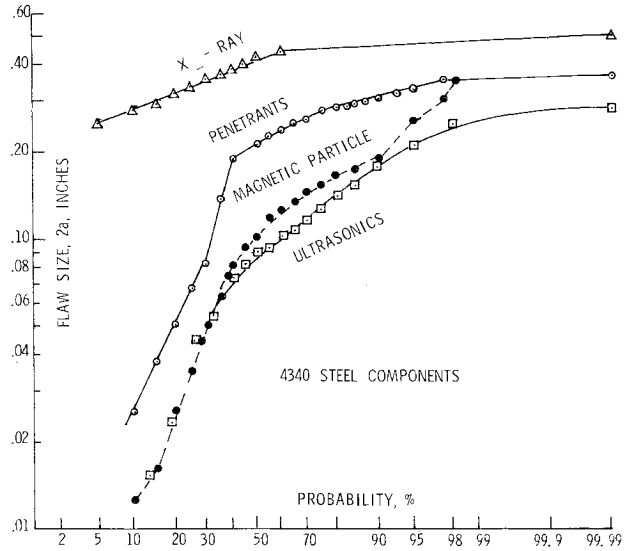

Fig. 13 Sensitivity of various nondestructive testing procedures for complex steel components.

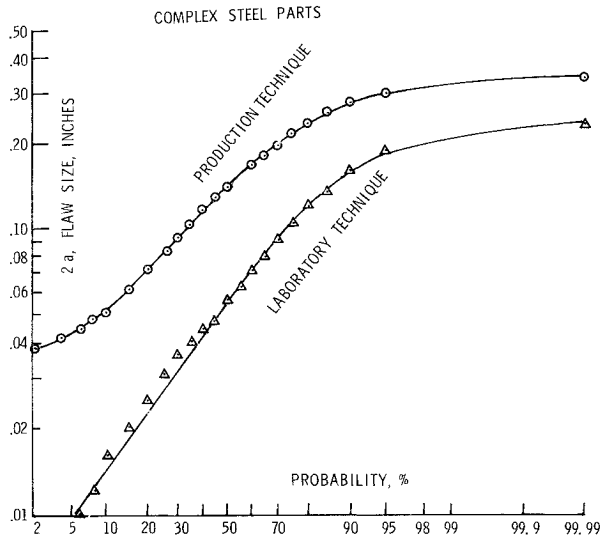

Fig. 14 Comparison of production and laboratory inspection techniques.

structive inspection and proof testing are obvious methods to cope with inherent defects. It is important to realize that nondestructive evaluation techniques can only detect small portions of the defects and moreover cannot resolve the absolute sizes. Each technique has a characteristic detectability curve which is governed by the materials, nature of the defect, component configuration, test procedures, and other factors. Obviously the chance of detecting a flaw increases for larger flaws. This is illustrated by Fig. 13, which displays the flaw size vs probability of detection characteristics[21] for various nondestructive evaluation techniques applied to steel components. Another aspect of the inspection process is illustrated by Fig. 14, representing typical results portraying the sensitivity of less costly production inspection procedures vs laboratory techniques employing highly trained and experienced personnel. The capabilities of nondestructive test methods have been evaluated for several metals,[38] and in addition limited data on inspection capabilities for structural ceramics is available.[39]

Using data similar to that illustrated in Fig. 13 and 14, appropriate for the materials and geometry of concern, the selection of materials can now be based on the estimated probability of occurrence of the particular flaw size, as well as the likelihood of detecting that particular flaw size. Material comparisons would be based on the overall probability, namely the product of the probabilities of existence of the critical flaw sizes and the likelihood of detecting the flaw. Obviously, the reliability of the methodology could be enhanced by multiple use of the various nondestructive evaluation techniques.

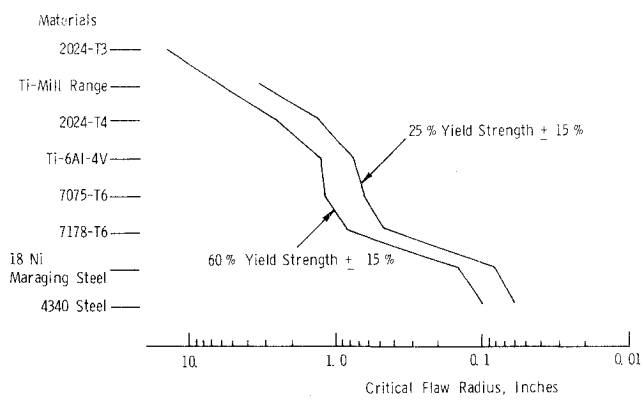

Fig. 15 Ranking of mean flaw radius for 60% and 25% yield stress levels.

Table 3

Material	Coefficient of variance % flaw radius: Design stress 60% Yield ± 15%	Coefficient of variance % flaw radius: Design stress 25% Yield ± 15%	Coefficient of variance % in.: Fracture toughness	Coefficient of variance % in.: Yield Strength
2024-T3	36.2	35.5	4.7	8.3
Ti-mill range	35.6	34.8	3.6	7.1
2024-T4	39.7	39.1	8.6	8.3
Ti 6Al4V	35.9	35.1	4.1	7.1
7075-T6	46.3	45.8	14.2	5.9
7178-T6	42.3	41.7	11.0	8.0
18 Ni maraging steel	36.6	35.8	5.1	6.9
4340 steel	36.7	36.0	5.2	6.25

Conclusions

It is important to employ probability-based materials selection criterion for several reasons. First, the critical flaw size estimates, for instance, involve a nonlinear equation, requiring multiple parameter input. Secondly, for these conditions, use of the Monte Carlo Method has demonstrated lack of linear proportionality of results, particularly when confidence limits are introduced into the materials optimization. Comparison of mean flaw estimates, for 25% and 60% operating stress levels is made in Fig. 15 and Table 3. There is a definite ranking which is merely shifted depending on the magnitude of the design stress. However, consideration of the 95% confidence levels, Fig. 16, for the stresses, indicates a considerable region of overlap which tends to obscure materials selection, and furthermore imposes the necessity for a more systematic evaluation of the influence of each controlling parameter in the fracture mechanics relation. That is, from the optimization viewpoint, one can isolate the controlling influence of each material property variability.

Also shown in Table 3 is the coefficient of variance, in percent, for the input values of fracture toughness and yield stress, along with the resulting coefficient of variance in mean flaw sizes. Note that the magnitude of variance is considerably larger than would result from application of a simple series approximation technique. The range of variance for the different materials is of interest. Steel, titanium and aluminum alloys exhibit coefficients of variance in defect radii ranging from about 35–46%. Referring to Fig. 6 for hot pressed beryllium, we see the corresponding range is 20–42% as the variance increases in the design stress from 0–15%. The hot pressed silicon nitride flaw estimates exhibit even more variability

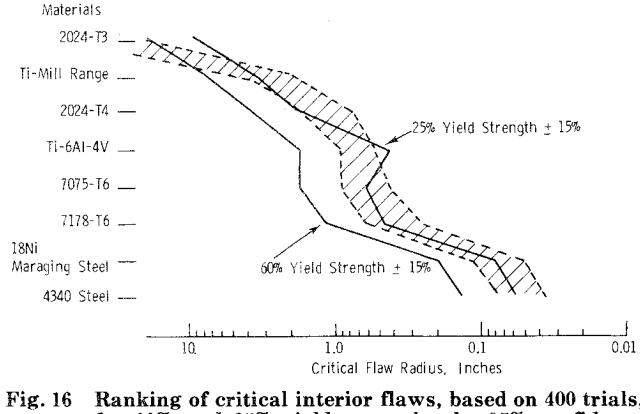

Fig. 16 Ranking of critical interior flaws, based on 400 trials, for 60% and 25% yield stress levels, 95% confidence limits.

(51–66%, as seen in Fig. 9), typifying a more brittle, less predictable response.

Referring to Tables 1 and 2, it is apparent that for a number of materials, the flaw size estimates were excessively large suggesting lack of brittle fracture susceptibility or perhaps an inapplicability of a simple Mode I fracture criterion. In the case of silicon nitride, flaw size estimates appeared to be of the correct order of magnitude in terms of inherent materials defects. While the defect estimates also appeared reasonable for 4340 steel and beryllium, it is important to recall the overriding importance of manufacturing techniques and process control in establishing the magnitude of inherent materials defect. In 4340 steel, for instance, it is known that the controlling microstructural defect can be modified by two or three orders of magnitude, merely by controlled vacuum as opposed to air melting.[40] The importance of surface integrity in defining the critical defect size relative to fatigue crack initiation is also well known in a number of materials. Thus metallurgical and process control aspects do contribute an equally important role in fracture-based materials selection.

Nonetheless, ability of the Monte Carlo method to treat variability in the multiparameter relationships of critical flaw size and crack growth rules is a distinct advantage over traditional deterministic approaches. Failure of simpler methods to represent variability in the solution is shown in Fig. 1 and Table 2. In Fig. 1 the mean values agree reasonably well for the two methods but the assumed normal distribution differs considerably from the Monte Carlo determinations. Table 2 shows generally poor agreement for the standard deviation over most of the range of variability in operating stresses.

With regard to application of the Monte Carlo method, this paper demonstrates that selection of the appropriate number of simulations must rely on consideration of third and higher order moments of the resulting statistical distributions. It was demonstrated that mean values and standard deviations were fairly constant after a relatively few trials, whereas the third and fourth moments continued to exhibit instability until considerably larger numbers of simulations had been completed.

In terms of fatigue life estimates, other forms of crack growth equations should be investigated. Crack growth data displayed on a log-log plot, usually exhibits a characteristic sigmoidal form and this as well as other representations must be studied carefully to obtain the most desirable methodology.

Further work is obviously required to fully verify the Monte Carlo methodology, particularly for elevated temperatures and response of complex engine components exposed to environmental extremes and representative spectrum loadings. Moreover it is certain that ceramic materials require further experimental and theoretical developments in order to achieve accurate component life estimate capabilities. In particular, more carefully evaluated test methods to determine crack growth rate parameters are especially important.

References

[1]Lin, A. F., "Statistical Variation in Fracture Toughness Data of Airframe Materials," AFFDL TR70-144, *Proceedings of the Airforce Conference on Fatigue and Fracture of Aircraft Structures and Materials,* Air Force Flight Dynamics Lab., Wright-Patterson Air Force Base, 1969.

[2]Campbell, J. E., Berry, W. E., and Feddersen, C. E., *Damage Tolerant Design Handbook,* MCIC-HB-01, Dec. 1972, Metals and Ceramics Information Center, Battelle Memorial Institute Labs., Columbus, Ohio.

[3]Shreider, Y. A., "The Monte Carlo Method," *International Series of Monographs in Pure and Applied Mathematics,* Vol. 87, Pergamon Press, New York, 1966.

[4]Benjamin, J. R. and Cornell, C. A., *Probability, Statistics and Decision for Civil Engineers,* McGraw-Hill, New York, 1970.

[5]"Stat Pack," Univac Division of Sperry Rand Corp., Advanced Computer Techniques Corp., New York,

[6]Sedlacek, R. and Jones, R. L., "A Study of Properties and Behavior of High Temperatures Gas Turbine Materials," Contract DAAG46-73-C-0206 AMMRC CTR. 74-19, March 1974, Stanford Research Institute, Palo Alto, Calif.

[7]Sedlacek, R. and Jones, R. L., "Mechanical Testing of Ceramic Rings," Cont. DAAG46-72-C-0112, May 1974,

[8]Baratta, F. I., Driscoll, G. W., and Katz, R. N., "Fracture Toughness," *Fractography and Finishing Effects in Silicon Nitride-Army, Materials Technology Conference,* Ceramics for High Performance Applications, 1973,

[9]Baumgartner, H. R. and Richerson, D. W., "Inclusion Effects on the Strength of Hot Pressed Si_3N_4," Pennsylvania State University Symposium on Fracture Mechanics of Ceramics, July 1973.

[10]Brown, W. F., Jr., "ASTM Standardization Activities in Fracture Testing of Beryllium Journal of Testing and Evaluation," *Journal of Testing and Evaluation,* Vol. 1, March 1973,

[11]Conrad, H., Hurd, J., and Woodard, D., "The Fracture Toughness of Beryllium," *Journal of Testing and Evaluation,* Vol. 1, March 1973, pp. 88–99.

[12]Jones, M. H., Bubsey, R. T., and Brown, W. F., Jr., "Crack Toughness Evaluation of Hot Pressed and Forged Beryllium," *Journal of Testing and Evaluation,* Vol. 1, March 1973, pp. 110–118.

[13]Shabbets, W. O. and Logsdon, W. A., "S-200 Grade Beryllium Fracture Toughness Properties," *Journal of Testing and Evaluation,* Vol. 1, March 1973, pp. 110–118.

[14]Hoeppner, D. W. and Krupp, W. E., *Prediction of Component Life Engineering Fracture Mechanics,* Vol. 6, Pergamon Press, New York, 1974, pp. 47–70.,

[15]Pelloux, R. M. N., "Review of Theories and Laws of Fatigue-Crack Propagation," AFFDL-TR 70-144, *Proceedings of the Air Force Conference on Fatigue and Fracture of Aircraft Structures and Materials,* Air Force Flight Dynamics Lab., Wright-Patterson Air Force Base, 1970, pp. 409–416.

[16]Barsom, J. M., "Review and Analysis of Fatigue—Crack Propagation Laws," Rept. 689.018-020, Vol. 5, 1969, United States Steel, Monroeville, Pa.

[17]Frost, N. E., Pook, L. P., and Denton, K., "A Fracture Mechanics Analysis of Fatigue-Crack Growth Data for Various Materials," Rept. Z 2/1/69, 1969, National Engineering Lab, England.

[18]Johnson, H. H. and Paris, P. C., "Subcritical Crack Growth," *Engineering Fracture Mechanics,* Vol. 1, Pergamon Press, New York, 1968,

[19]Freudenthal, A. M., "Fatigue and Fracture Mechanics," *Engineering Fracture Mechanics,* Vol. 5, Pergamon Press, New York, 1973, pp. 403–414.

[20]Kula, E. and Anctil, A. A., "Effects of Environment and Complex Load History on Fatigue Life," ASTM-STP-462, 1970 American Society for Testing and Materials, Philadelphia, Pa., pp. 297–317.

[21]Krupp, W. E. and Hoeppner, D. W., "Fracture Mechanics Application in Materials Selection, Fabrication Sequencing and Inspection," *Journal of Aircraft,* Vol. 10, Nov. 1973, pp. 682–688.

[22]Evans, A. G. and Wiederhorn, S., "Crack Propagation and Failure Prediction in Silicon Nitride at Elevated Temperatures," *International Journal of Fracture Mechanics,* to be published.

[23]Williams, D. P. and Evans, A. G., *Journal of Testing and Evaluation,* Vol. 1, 1973, p. 264.

[24]Evans, A. G., "A Simple Method for Evaluating Slow Crack Growth In Brittle Materials," *International Journal of Fracture,* Vol. 9, Sept. 1973,

[25]Evans, A. G., "Slow Crack Growth in Brittle Materials Under Dynamic Loading Conditions," *International Journal of Fracture,* Vol. 10, June 1974, pp. 251–261.

[26]Evans, A. G., Russel, L. R., and Richerson, D. W., "Slow Crack Growth and Failure Predictions at Elevated Temperatures," to be published.

[27]Evans, A. G. and Wiederhorn, S., "Proof Testing of Ceramic Materials An Anlaysis Basis for Failure Prediction," *International Journal of Fracture,* to be published.

[28]Weibull, W., "A Statistical Theory of the Strength of Materials," *Proceedings of the Ingeniors Vetenskaps Akademien,* Vol. 151, Jan. 1939.

[29]Freudenthal, A. M., "Statistical Approach to Brittle Fracture," Ch. 6, *Fracture, An Advanced Treatise, Vol. II, Mathematical Fundamentals,* edited by H. Liebowitz, Academic Press, New York, 1968, pp. 591–618.

[30]Gilvarry, J. J., "Fracture of Brittle Solids I. Distribution Function for Fragment Size in Single Fracture (Theoretical)," *Journal of Applied Physics,* Vol. 32, March 1961, pp. 391–399.

[31]McClintock, F. A., "Preliminary Reports, Memoranda and Technical Notes of the Materials Research Council, Summer Conference," Vol. I, July 1973, Advanced Research Projects Agency, LaJolla, Calif.

[32]Oh, H. L. and Finnie, I., "On the Location of Fracture in Brittle Solids, I, II," *International Journal of Fracture Mechanics,* Vol. 6, Dec. 1970, pp. 287 and 339.

[33]Batdorf, S. B. and Crose, J. G., "A Statistical Theory for the Fracture of Brittle Structures Subjected to Nonuniform Polyaxial Stresses," *Journal of Applied Mechanics,* Vol. 41, June 1974.

[34]Batdorf, S. B., "Fracture Statistics of Brittle Materials with Intergranular Cracks," Rept. SAMSO-TR-74-210, Oct. 1974, Space & Missile Systems Organization, Air Force Systems Command, Los Angeles, Calif.

[35]Lenoe, E. M. and Baratta, F. I., "Recent Studies Towards the Development of Procedures for the Design of Brittle Materials," *Proceedings of the Colloquium on Structural Reliability: The Impact of Advanced Materials on Engineering Design,* 1972, Carnegie Mellon Univ., 1972, pp. 433–462.

[36]Batdorf, S. B., private communication, April 1974, Las Vegas, Nev.

[37]Tang, W. H., "Probabilistic Updating of Flaw Information, *Journal of Testing and Evaluation,* Vol. 1, Nov. 1973, pp. 459–467.

[38]Lord, R. J., "Evaluation of the Reliability and Sensitivity of NDT Methods for Titanium Alloys," Tech. Rept. AFML-TR-73-107, Vols. I and II, March 1974, Air Force Materials Lab., Wright-Patterson Air Force Base, Ohio.

[39]Beck, R. J. "Evaluation of Ceramics for Small Gas Turbine Engines," Paper 740239, Feb.–March 1974, Automotive Engineering Congress, Detroit, Mich.

[40]Papirno, R., "Cyclic-Time History of Fatigue Crack Initiation in Vacuum Melted 4340 Steel," *Metallurgical Transactions.*